

YouLighter: A Cognitive Approach to Unveil YouTube CDN and Changes

Original

YouLighter: A Cognitive Approach to Unveil YouTube CDN and Changes / Giordano, Danilo; Traverso, Stefano; Grimaudo, Luigi; Mellia, Marco; Baralis, ELENA MARIA; Tongaonkar, Alok; Saha, Sabyasachi. - In: IEEE TRANSACTIONS ON COGNITIVE COMMUNICATIONS AND NETWORKING. - ISSN 2332-7731. - ELETTRONICO. - 1:2(2015), pp. 161-174. [10.1109/TCCN.2016.2517004]

Availability:

This version is available at: 11583/2640333 since: 2019-08-23T14:28:56Z

Publisher:

IEEE

Published

DOI:10.1109/TCCN.2016.2517004

Terms of use:

This article is made available under terms and conditions as specified in the corresponding bibliographic description in the repository

Publisher copyright

IEEE postprint/Author's Accepted Manuscript

©2015 IEEE. Personal use of this material is permitted. Permission from IEEE must be obtained for all other uses, in any current or future media, including reprinting/republishing this material for advertising or promotional purposes, creating new collecting works, for resale or lists, or reuse of any copyrighted component of this work in other works.

(Article begins on next page)

YouLighter: A Cognitive Approach to Unveil YouTube CDN and Changes

Danilo Giordano¹, Stefano Traverso¹, Luigi Grimaudo¹,
Marco Mellia¹, Elena Baralis¹, Alok Tongaonkar², Sabyasachi Saha³

¹Politecnico di Torino - first.last@polito.it

²Symantec Corporation - alok_tongaonkar@symantec.com

³Cyphort - sabyasachi.saha@gmail.com

(Invited Paper)

Abstract—

YouTube relies on a massively distributed Content Delivery Network (CDN) to stream the billions of videos in its catalog. Unfortunately, very little information about the design of such CDN is available. This, combined with the pervasiveness of YouTube, poses a big challenge for Internet Service Providers (ISPs), which are compelled to optimize end-users' Quality of Experience (QoE) while having almost no visibility and understanding of CDN decisions.

This paper presents *YouLighter*, an unsupervised technique that builds upon cognitive methodologies to identify changes in how the YouTube CDN serves traffic. *YouLighter* leverages only passive measurements and clustering algorithms to group caches that appear co-located and identical into *edge-nodes*. This automatically unveils the YouTube edge-nodes used by the ISP customers. Next, we leverage a new metric, called *Pattern Dissimilarity*, that compares the clustering results obtained from two different time snapshots to pinpoint sudden changes.

By running *YouLighter* over 10-month long traces obtained from two ISPs in different countries, we pinpoint both sudden changes in edge-node allocation, and small alterations to the cache allocation policies which actually impair the QoE that the end-users perceive.

Index Terms—Network Monitoring, Clustering, YouTube

I. INTRODUCTION

YouTube is one of the most popular and demanding Internet services. It accounts for 1 billion users distributed world-wide, who watch 6 billion hours of videos per month.¹ Due to its popularity and the nature of the content that it distributes, the demanded load to handle is huge, and guaranteeing a satisfactory Quality of Experience (QoE) for the users is a challenging task to accomplish. To this end, YouTube leverages a massive, globally distributed Content Delivery Network (CDN), the Google CDN [1]. It consists of hundreds of *edge-nodes* scattered in the Internet. Each edge-node hosts hundreds of video servers, or *caches*, which can each potentially serve any video any user may request [2].

Google, as many other Over-the-Top content providers, places its edge-nodes close to users, usually at aggregation

points directly peering with Internet Service Providers (ISPs).² Hence, Google uses the ISP's network as the "last mile" to deliver YouTube videos. Despite this localized setup, once a user requests a video playback, the CDN load balancing algorithm directs the request to one of the caches, and there is no mean to predict which cache, or even which edge-node will be used [3], [4]. This is particularly critical for the ISP, which on the one hand is compelled to deliver YouTube videos to the customers without impairing the QoE, while on the other aims at minimizing the delivery costs. Hence, the ISP spends a significant effort in monitoring the CDN infrastructure and designing ad hoc traffic engineering policies for YouTube traffic [5]. However, the YouTube CDN allocation policy frequently changes caches being used to serve videos, and changes may involve modifications in the infrastructure, e.g., the activation of a new cache, or in the load balancing algorithm decision, e.g., a sudden switch of caches to serve requests, or an eventual change on the path to those caches, e.g., due to congestion, or route change. Conversely, the ISP's policies are often static and hardly cope with the continuous evolution of the Google CDN: any sudden change can make the ISP's optimization obsolete, and thus ineffective, possibly causing abrupt disruptions or QoE degradations. This constitutes an issue for the ISP, as it sees its reputation degrade when a change happens, even if Google caused it.

A. Our Contribution

In this paper, we present *YouLighter*, a novel methodology to automatically monitor and pinpoint changes in how the YouTube CDN serves traffic. *YouLighter* relies on an unsupervised learning approach that, as such, does not require any knowledge of the YouTube infrastructure. It builds upon a cognitive approach, where automatic and unsupervised algorithms are used to extract a model of the system status. *YouLighter* only assumes that the ISP has deployed passive traffic probes, which expose TCP flow level logs summarizing video requests from users. Considering a given observation window of, say one day, *YouLighter* aggregates these flow logs to constitute a *snapshot* of the traffic exchanged with YouTube caches. Based on DBSCAN [6], a well-established unsupervised machine learning algorithm, *YouLighter* is able to automatically group

A preliminary version of this paper has been presented at the 27th International Teletraffic Congress (ITC27)

The research leading to these results has received partial funding from the European Union under the FP7 Grant Agreement n. 318627 (Integrated Project "mPlane") and partially from Narus Inc., Sunnyvale, CA.

¹<https://www.youtube.com/yt/press/statistics.html>

²<https://peering.google.com/about/index.html>

thousands of caches into a bunch of edge-nodes using simple features that characterize the network distance of caches from the vantage point.

YouLighter periodically runs DBSCAN on consecutive snapshots, extracting for each of them a model of the status of the CDN. The problem becomes then how to compare the two models to highlight eventual changes. We solve it with some ingenuity, we summarize the corresponding models into *patterns*, and compare them using the notion of *Pattern Dissimilarity*, a metric similar to others presented in the literature, but which satisfies our specific requirements (see Sec. II for a detailed discussion). The bigger the distance between two snapshots is, the more different the sets of YouTube caches to serve ISP customers during the two periods of time are.

YouLighter highlights several kinds of changes, including deviations from the typical behavior of edge-nodes possibly induced by congestion arising in the network. In general, *YouLighter* triggers alarms corresponding to sudden changes happening in the YouTube CDN infrastructure which may be responsible of QoE issues for ISP customers. Resulting alarms are then offered to the ISP network administrator who can take countermeasures to mitigate the problem.

We validate our methodology over traces we collect from four different vantage points that we have deployed in two ISPs in two different countries. First, we demonstrate that the cognitive algorithms *YouLighter* adopts are effective at identifying and grouping YouTube caches belonging to different edge-nodes. Second, we run *YouLighter* over different collected snapshots considering a longitudinal dataset, which, overall, accounts for more than 33 months of traffic. We pinpoint several examples of sudden and previously undiscovered changes in the YouTube CDN. For some of them, we investigate the impact on the QoE of ISP customers, revealing the sudden drop of average video download throughput to less than 250 kb/s, which hampers even the possibility of watching a video.

We believe that *YouLighter* is a promising tool for ISPs, network administrators and researchers to monitor the YouTube CDN and the traffic it generates. Importantly, thanks to its design, *YouLighter* offers the capability of automating and accelerating the troubleshooting procedures. In fact, ISPs may use *YouLighter* to quickly react to changes possibly harming customer's QoE. For instance, ISPs may adopt traffic engineering algorithms to optimize routing to under-performing edge-nodes, e.g., by means of BGP policies, or to implement DNS policies overruling YouTube choices and re-directing traffic from caches with bad QoE to changes with a good QoE. However, *YouLighter's* task is limited to notifying the occurrence of change events in the YouTube CDN. The investigation and troubleshooting of issues notified by *YouLighter* are out of the scope of this paper.

The remainder of this paper is structured as follows: Sec. II discusses the related work. Sec. III describes the details of our datasets, and shows the dynamicity of YouTube cache selection policies. Sec. IV presents our methodology, introduces the notion of *Pattern Dissimilarity*, and discusses *YouLighter's* complexity. Sec. V presents our results: First, we evaluate the sensitivity of *YouLighter's* parameters, and, second, we

show how effective *YouLighter* is at pinpointing changes in YouTube CDN employing our traces. Sec. VII suggests some countermeasures an ISP can use to improve users' QoE in case of changes. Finally, Sec. VIII concludes the paper.

II. RELATED WORK

A large body of work has analyzed the YouTube delivery infrastructure and its evolution over time [1], [2], [3], [7], [5]. They show YouTube is a highly dynamic system which keeps changing over time due to continuous upgrades in the infrastructure [1], [2] or due to the dynamicity of the cache selection policies [3], [7]. Some of the findings are already outdated. For instance, the load-balancing policy based on HTTP redirections which is described in [3], [7] is no longer in place, and YouTube dismissed the naming scheme described in [2] at the end of 2011. In this work, we do not aim to offer an updated view or characterization of YouTube. Instead, we present a methodology that allows to automatically identify changes in both the infrastructure, e.g., the appearance of new edge-nodes, and in the day to day management of the infrastructure, e.g., a change in the load-balancing algorithm that may affect millions of customers.

Our contribution is in line with the body of works focusing on anomaly detection, for which [8], [9] offer good surveys. In particular, our work belongs to the family of studies which addresses the problem of performing anomaly detection in large scale operational networks. [10], [11] are notable examples of supervised methodologies which leverage data from passive probes, topology information, routing tables and Simple Network Management Protocol (SNMP) logs to match predictions to actual measurements to pinpoint deviations.

Other works propose methodologies to perform anomaly detection on CDN infrastructures for video delivery specifically [12], [13], [5]. Authors of [12] consider a collection of video download sessions, out of which they extract measurements for specific features, and manually set thresholds to label degradation-affected sessions. Then, by applying graph techniques, they identify clusters and outliers possibly associated to performance issues. [13] analyzes different CDN providers, among which YouTube. The paper presents a characterization of the YouTube cache selection policy and apply an anomaly detection system based on subnet usage to detect unexpected cache selection in a time window of minutes. Finally, [5] focuses on the YouTube case too and proposes a methodology for anomaly detection which requires a significant manual effort, and the paper mostly presents results about the characterization of the YouTube service in terms of traffic characteristics and QoE perceived by the users. *YouLighter* differs from the supervised methodologies described in above studies. In fact, *YouLighter* does not assume any knowledge of a baseline, and leverages unsupervised algorithms to automatically unveil changes on the YouTube infrastructure. We design it with this specific requirement in mind, as it has to target the YouTube CDN, for which the ground truth is a moving target that is very difficult to know.

The application of cognitive and unsupervised machine learning techniques – in particular clustering techniques – to

perform anomaly detection based on network traffic is not new. For instance, [14] proposes a flow-based anomaly detection algorithm based on K-Means, while [15] uses DBSCAN to group P2P sessions and identify anomalous clusters. However, in all the cases, clustering is used to study the same given dataset. Our goal is anomaly detection algorithm builds on the comparison between clustering patterns obtained at different times. The task of identifying anomalies by comparing clustering results attained from different datasets (e.g., different time snapshots, etc.) translates in the problem of measuring the dissimilarity of two distinct patterns. The comparison and quantification of the similarity obtained from evolving-in-time clustering is addressed within a sub-domain referred to as *online clustering* or *streaming clustering*. See [16], [17] for notable examples. In particular, [16] defines a metric to quantify the dissimilarity between consecutive clustering patterns, namely the History Cost, which is similar to the Pattern Dissimilarity presented in this work. However, the History Cost is designed to compute the distance between clustering patterns built by K-Means, for which the number of clusters is constant across different patterns. Instead, the Pattern Dissimilarity takes into account the case in which the number of clusters across different patterns is different. Another work which goes in a similar direction is [18] whose authors propose to measure similarity between sets of overlapping clusters from complex networks, in which groups of nodes form tightly connected units linked to each other. Since points are not embedded in a metric space, authors of [18] define ad-hoc distances.

YouLighter differs also from techniques for the tracking of moving clusters and objects as in [19], [20]. Indeed, their goal is to track the movements of the same clustered objects over time, e.g., a group of migrating animals. On the contrary, *YouLighter* has no insights about the CDN infrastructure and it cannot track single objects, which may disappear and reappear freely.

Finally, other approaches as [21] measure the similarity among sample distributions obtained at different time intervals. However, directly relying on distributions to perform the comparison considerably complicates the detection of the edge-nodes behind the changes. And from the datamining community evolutionary clustering techniques such as [16], [17] have been used to study how clustering results evolve over time. Instead, *YouLighter* extracts and compares clustering patterns, which are simpler to process in an automatic manner, and allow to immediately pinpoint the edge-nodes (i.e., the clusters) responsible for possible deviations.

A preliminary version of this work has been presented [22]. In this extended version we present more thorough performance analysis and sensitivity study of *YouLighter* algorithms, present a complexity evaluation and discuss possible counter-measures ISP can take to mitigate eventual problems.

III. DATASETS

We assume the ISP has instrumented the network with passive probes, which collect statistics from traffic flows carrying YouTube videos. In this work, we rely on passive

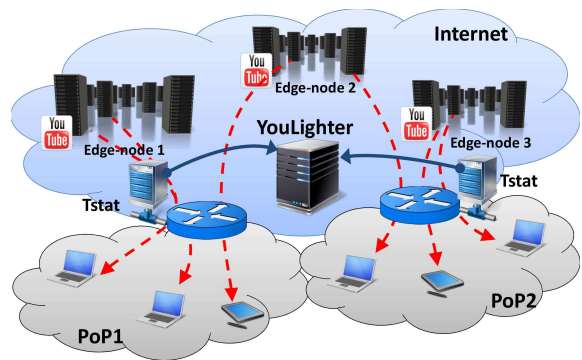


Fig. 1: The traffic monitoring setup we employ for this paper.

probes running Tstat³ that we install in Points-of-Presences (PoPs) of operational networks, as depicted in Fig. 1. Clients are located in one PoP, and connect to the backbone via a router, where Tstat monitors the traffic. Tstat observes packets, rebuilds each TCP flow, tracks it, and at the end of the flow, logs detailed statistics. Tstat can classify TCP flows that carry YouTube videos. For each request, it logs i) the anonymized client IP address, ii) the server IP address, iii) the hostname of the server,

iv) the TCP minimum Round Trip Time (RTT), v) the IP Time-To-Live (TTL) of packets received by the client in the PoP, vi) the amount of bytes the clients send and receive, vii) the average download throughput, and viii) the time at which the TCP connection starts.⁴ For more information we address the reader to [23]. Note that Tstat can compute all these metrics considering only TCP segments, and do not require access to application payload. On the one hand, this avoids any privacy issues. And other hand, it allows us to collect all needed statistics even in presence of encryption, e.g. when HTTPS is used, which nowadays represents more than 50% of overall YouTube traffic [24].

Trace	Period	Volume	Flows	Caches
ISP1-A	01/04/2013 - 28/02/2014	138.7 TB	33,216,794	8,664
ISP1-B	01/04/2013 - 28/02/2014	152.9 TB	31,643,603	8,899
ISP1-C	01/04/2013 - 28/02/2014	134.8 TB	27,377,089	9,028
ISP2	01/03/2014 - 17/07/2014	48.3 TB	9,100,163	3,755

TABLE I: Traces considered in this study.

We have been collecting traffic logs since April 2013 by monitoring the traffic users generate when accessing the Internet. We instrument four different PoPs. Three of them are located in networks of the same ISP, and in two different cities of the same country. We install the fourth one in a PoP of a different ISP in a second country. Tab. I describes, for each trace (or dataset), the time period, the total downloaded volume, the number of unique videos and the number of YouTube servers we observe. Notice that in total we monitor the activity of more than 32,000 customers, and the maximum

³<http://www.tstat.polito.it>

⁴The RTT is measured as the time difference between the server acknowledgement segment and the corresponding client data segment. Give a TCP connection, the minimum RTT is computed among all valid samples. The TTL is directly extracted from the IP header. Among all packets in a flow, we take the minimum value seen.

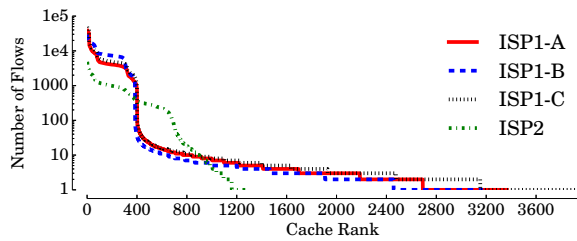


Fig. 2: Rank of YouTube caches based on the number of flows. February 2014, *ISP1*.

number of YouTube caches that *ISP1* customers used at least once is $\sim 9,000$. The dataset overall covers more than 500 TB of equivalent data.

A. YouTube Cache Naming Structure

We find that the YouTube infrastructure described in [2] is no longer in use. During 2012, YouTube server hostnames were in the form $rx---ABCxxtxx.c.youtube.com$, where x are numbers, while ABC is a three-letter code reporting the International Air Transport Association (IATA) code of the closest airport. For instance $r7---fra07t16.c.youtube.com$ identified a single cache, in Frankfurt. The hostname still resolves to a single IP address, 74.125.218.182 in the example. Thus, we can uniquely identify a cache by its hostname.⁵ All caches co-located in the same edge-node share the same (obfuscated) IATA code. This allows us to get coarse ground truth about the location of servers.

We run some active experiments to cross-check if YouTube specializes caches to serve some particular content, and we verify that every cache can serve any video, at any resolution, in any format, e.g., MPG4 or Flash, to any device, e.g., PC, smartphones or tablets.

B. Characterization of the Load Balancing Policies

Every time a user starts a video playback, the player starts a progressive download of the video content from the specific cache the system provides in the HTML page.⁶ We are interested in seeing which are the policies governing the server allocation, such as (i) is there any “preferred” group of caches? or (ii) are those stable over time?

Fig. 2 reports the rank of YouTube caches sorted by the number of flows they serve. We consider February 2014 from the *ISP1* datasets. First, notice that we observe up to 3,800 in *ISP1-C*, with *ISP1-A* reaching more than 2,500. Second, the load each cache handles is very heterogeneous in all datasets; few servers handle lots of requests, but there is a not negligible

⁵Starting from January 2013, YouTube obfuscates the IATA code using a simple substitution cipher. The script to de-obfuscate YouTube encrypted cache names is available at http://tstat.polito.it/svn/software/tstat/trunk/scripts/decode_yt_sitename.pl. From October 2013, the *youtube.com* domain has been replaced by the *googlevideo.com* domain. This information can be used to identify YouTube flows even in presence of HTTPS [25].

⁶Load balancing policies are implemented at application layer. Indeed, the web server chooses and encodes the cache hostname directly in the HTML page served to the client.

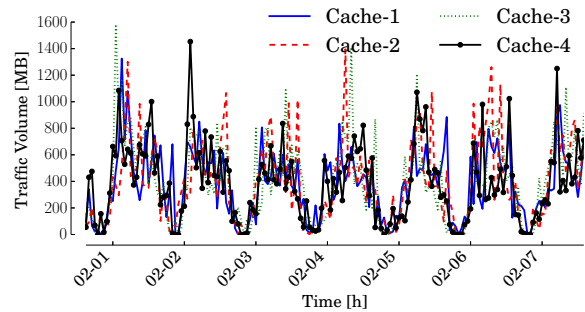


Fig. 3: Evolution of the volume of traffic for the four most active caches we observe on February 1st 2014. First week of February 2014, dataset *ISP1-A*.

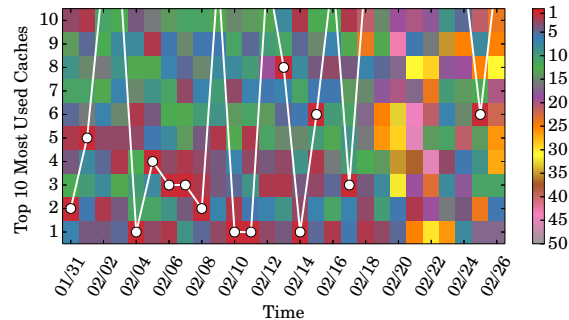


Fig. 4: Evolution over time of the rank of the top 10 mostly used caches during February 2014, *ISP1-A*. The white dot corresponds to the top cache of each day.

number of caches that serves a significant portion of flows. In all three datasets, top 400 caches serve more than 1,000 videos, and, to observe 95% of requests, one must consider about 313, 330, 342 caches in *ISP1-B*, *ISP1-A*, *ISP1-C* respectively.

We also notice that the rank is extremely dynamic over time. For instance, we pick randomly four caches among the most active caches in *ISP1-A* during the 1st week of February 2014. We report in Fig. 3 the amount of traffic they generate over time for the following seven days. As shown, the amount of traffic a single cache handles changes widely over time, and none of the monitored caches keeps a constant leading position for a long period of time.

As one may expect this dynamicity to disappear when reducing the focus, we monitor a larger pool of caches as those in the rank in Fig. 2, and we recompute the same rank on a daily basis. Then, we represent it using different colors in Fig. 4. Each row represents the rank of the same cache for different days in February. In case the rank is stable, one would expect a row (a cache) to always assume the same color (rank). Fig. 4 shows exactly the opposite. Indeed the top daily cache (red square, highlighted by the white dot) randomly changes every day (white line). Sometimes, the most used cache in a day is not among the top-10 cache of the month (line jumps outside). The top-10 caches in the monthly rank drops below the 50th place during some days (gray color). Similarly, in the first 19 days of February, the top-10 caches are concentrated in the first 20 rankings; However, starting from February 20th they fall around the 30th position (notice the concentration of

yellow and orange boxes).

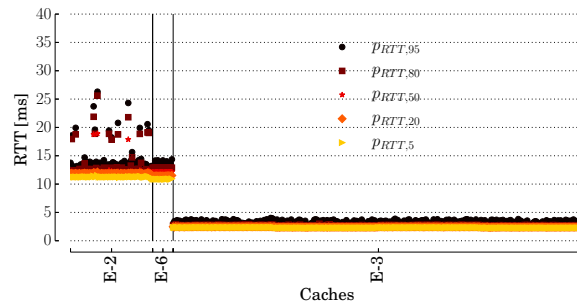
This shows that the server allocation policies adopted by YouTube spread the load over several hundreds of caches, and the choices are extremely dynamic over time if we observe with the fine grained granularity of a single cache.

Since caches inside the same edge-node are all equivalent, the intuition is to observe the system using the coarse granularity offered by edge-nodes. However, edge-nodes are unknown, they can change over time due to system upgrade, maintenance operations, or redesign. Information that could be available (e.g., the IATA code) may be not reliable, or may be outdated by YouTube. This calls for cognitive systems that can automatically identify presence of edge-nodes and to build a model of the current status of the CDN. We thus design an unsupervised machine learning algorithm to automatically identify edge-nodes from just the observation of traffic flows.

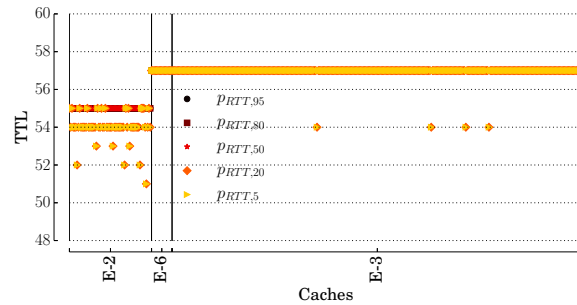
IV. METHODOLOGY

Among cognitive approaches that try to extract models out of data, cluster analysis (or clustering) represents a well known set of unsupervised algorithms that have been successfully used in the literature. Clustering algorithms group objects with similar characteristics [26]. Objects are described by means of features which map each object to a specific position in a hyperspace. The similarity between two objects is based on their *distance*. The closer the two objects are, the more likely they are similar and thus should be grouped in the same cluster. Typically, the Euclidean distance is used.

The selection of the features plays a key role in the design of clustering algorithms. In our scenario we would like to group together caches based on the network position as seen from a vantage point. Intuitively, the path between two caches in the same edge-node and clients in the same PoP exhibits the same properties, that from a network perspective translates in same RTT and TTL. Conversely, the paths between two caches in two different edge-nodes should present different RTT or TTL. To confirm this intuition we perform the following experiment. We consider three edge-nodes observed in *ISP1-A* during December 12-18 2013. For each cache, we consider all the flow directed to it and we compute the Cumulative Distribution Function (CDF) of the RTT and the TTL extracted from the flows. Then we summarize each CDF with the 5th, 20th, 50th, 80th, and 95th percentiles, and report the result in Fig. 5. The x axis reports caches grouped together by (anonymized) IATA code. On the y axis, for each cache, we report the percentile values, shaded with different colors, obtained from the per-cache CDFs. Fig. 5(a) and Fig. 5(b) reports the results for RTT and TTL, respectively. Since we sort caches based on their IP address and IATA code, caches belonging to the same edge-node appear one close the other. Three edge-nodes are present, E-2, E-6, and E-3. Each hosts a variable number of caches, with E-3 being the largest. As shown in Fig. 5(a), the caches in the same edge-node exhibits very similar RTT percentiles, suggesting that we can identify clusters of caches by considering the RTT as a feature. However, E-2 and E-6 exhibit very similar RTT percentile values. This fact clearly complicates the capability



(a) RTT percentiles



(b) TTL percentiles

Fig. 5: Example of per-cache RTT percentiles and TTL percentiles. Caches sorted by IP address, and grouped by (anonymized) IATA code. December 12-18 2013, dataset *ISP1-A*.

of a clustering algorithm to label them as different edge-nodes. Similarly, when focusing on the TTL (Fig. 5(b)) we observe that E-6 and E-3 show practically identical values. However, if we put Fig. 5(a) on top of Fig. 5(b), we can easily distinguish the three edge-nodes as they all exhibit different RTT and TTL combinations, and E-2, E-3 and E-6 emerge clearly as different edge-nodes. This simple example justifies our choice to consider the multidimensional space obtained by combining percentiles for both RTT and TTL features.

We acknowledge that The RTT and TTL samples might be biased by issues due to the presence of congestion in the network path to the caches. However, YouLighter's aim is to capture these kind of events as well, and notify them to the ISP, which then will investigate further to troubleshoot the problem. Anyhow, the correct working point of an ISP network should be far from a regime affected by congestion, so we expect congestion events to be due to actual changes in the CDN infrastructure or in the network paths to the caches, rather than in the ISP network.

A. Multi-dimensional Clustering

We leverage above intuition to design a clustering algorithm to automatically find homogeneous groups of caches. We use some ingenuity to characterize the path from client to each cache, and then to cluster caches that exhibits similar paths. We can split the process of our methodology into the following steps:

Step 1 - Passive monitoring of YouTube video flows: As described in Sec. III, a passive probe provides the continuous collection of YouTube traffic logs. We log the metadata of each TCP connection, and we store logs in a database for further processing.

Step 2 - Measurement consolidation and filtering: To ease the monitoring procedure, we use a batch processing approach that considers time windows of size ΔT . Thus, every ΔT we generate a “snapshot”, and we aggregate and process measurements in it. In the following, we indicate the n -th snapshot as a superscript when needed, e.g., $a^{(n)}$ indicates the metric a at snapshot n . The choice of the time granularity at which a new snapshot is built is driven by the necessity of finding a trade off between the amount of data to consider, and the frequency at which the network administrator is expected to be capable of reacting to anomalies.

We identify each cache x by its IP address. We then group all flows in the same snapshot with the same server IP address to obtain a table where columns correspond to the metric (e.g., RTT, TTL, transmitted packets, etc.), and each row corresponds to a sample, i.e., the tuple of measured values observed within a TCP flow.

Since we are interested in the active caches, we discard those with less than $MinFlow = 50$ samples. We define the whole measurement snapshot n as $X^{(n)}$.

Step 3 - Feature selection and data normalization: Next, we apply a feature selection driven by domain knowledge to select the set \mathcal{M} of *metrics*. In particular, as we are interested in grouping caches according to the path properties, we choose $\mathcal{M} = \{RTT, TTL\}$. Then, for each cache x in the snapshot X , and for each metric $m \in \mathcal{M}$, we generate a Cumulative Distribution Function (CDF). From the distribution, we extract the vector $P_m(x) = (p_{m,1}(x), p_{m,2}(x), \dots, p_{m,k}(x))$ containing k percentiles of m for cache x . Then, we translate the percentile values obtained from the real space to an hypercube space of unitary size. This is a standard approach which allows the data analytics algorithm to work with a fixed parameter configuration. We thus standardize percentiles following a simple normalization:

$$min_m = \min(p_{m,i}(x) \forall x \in X, \forall i = 1, \dots, k) \quad (1)$$

$$max_m = \max(p_{m,i}(x) \forall x \in X, \forall i = 1, \dots, k) \quad (2)$$

$$\bar{p}_{m,i}(x) = \frac{p_{m,i}(x) - min_m}{max_m - min_m} \quad (3)$$

Intuitively, Eq.(3) normalizes the percentiles of metric m so that $\bar{p}_{m,i} \in [0, 1]$.

At last, $\bar{P}_m(x) = (\bar{p}_{m,1}(x), \bar{p}_{m,2}(x), \dots, \bar{p}_{m,k}(x))$ represents the standardized vector of *features* for the metric m for server x . Recalling that $\mathcal{M} = \{RTT, TTL\}$, we identify each cache $x \in X$ with a $2k$ -dimensional **which is then normalized in a space of edge 1 and features**:

$$\bar{x} = (\bar{P}_{RTT}(x), \bar{P}_{TTL}(x)) \quad (4)$$

and we transform the original set of caches X into a set of points $\bar{X} = \{\bar{x}\}$.

Step 4 - Clustering: Among different clustering algorithms we employ the DBSCAN (Density-Based Spatial Clustering

of Applications with Noise) algorithm [6] to group together caches based on their multi-dimensional features. We choose DBSCAN because (i) it is able to handle clusters of arbitrary shapes and sizes; (ii) it is relatively resistant to noise and outliers; (iii) it does not require the specification of the number of desired clusters (iv) it is a density based clustering algorithm which perfectly fits our scenario. DBSCAN is a clustering algorithm presented in 1996 [6] which exploits the notion of dense area to clusterize elements. This characteristic is particularly useful in our scenario since caches belonging to the same edge-node should own similar metrics value lying in a small region of the possible space. Even in presence of small difference within the same edge-node, DBSCAN has good performance as it can handle clusters of different shape. Another important point is that DBSCAN requires only two parameters: ϵ and $MinPts$. ϵ determines the maximum allowed distance between any given point in a cluster and its closest neighbour belonging to the same cluster, and $MinPts$ the minimum number of points required to form a cluster. Based on that, it classifies all points as being (i) core points, i.e., in the interior of a dense region; (ii) border points, i.e., on the edge of a dense region; or (iii) noise points, i.e., in a sparsely occupied region. Noise points do not form any cluster, while the algorithm puts in the same cluster any two core points that are within ϵ of each other. Similarly, any border point that is close enough to a core point is put in the same cluster as the core point. The result of this process is a collection \mathcal{C} of clusters $C_j \in \mathcal{C}$, also named as *clustering*:

$$\mathcal{C} = \{C_j\} = \text{DBSCAN}(\bar{X}) \quad (5)$$

B. Highlighting Changes with the Pattern Dissimilarity

We are now interested in tracking the evolution of clusters over time, for which, we adapt the methodology presented in [16], as we discuss in Sec. I. As authors presented in [16] compare two clusterings $\mathcal{C}1$ and $\mathcal{C}2$ obtained considering two *different* datasets, i.e., snapshots in our case opens many different scenarios. For instance, i) points that were present in $\mathcal{C}1$ may not be present in $\mathcal{C}2$, and vice versa; ii) points clustered into the same cluster in $\mathcal{C}1$ can now belong to two or more clusters in $\mathcal{C}2$; and iii) the same points that form a cluster in $\mathcal{C}1$ can still form the same cluster, but can be placed in another region in the clustering space in $\mathcal{C}2$. In our case, this corresponds to i) popular caches at snapshot n that are not anymore used at snapshot $n + 1$, or ii) some caches at snapshot n that were part of the noise are instead clustered at snapshot $n + 1$, or iii) the path to caches suddenly changes at snapshot $n + 1$, altering RTT and TTL. Since we do not have any mean to label the clusters in two different clustering results for instance by using a ground truth label. We can not evaluate major changes, i.e., the presence of a totally new cluster by simply evaluating the difference of clustering results by comparing which clusters are shared between the snapshots. Therefore, to evaluate the difference between the clustering, we adapt the historic cost function presented in [16], and we introduce the notion of *Pattern Dissimilarity*.

1) *Clustering Patterns:* We first map each cluster into a single *Centroid* that summarizes it. For each cluster, a

centroid is computed following the standard approach, i.e., it is the mean position of all the points in all of the coordinate directions. Therefore, given a cluster $C \in \mathcal{C}$, we consider the centroid, or geometric center, \hat{x} whose components $\hat{p}_{m,i}$ in the i percentile of feature m are:

$$\hat{p}_{m,i} = \frac{1}{|C|} \sum_{x \in C} \text{renorm}(p_{m,i}(x)) \quad (6)$$

All centroids then form a *pattern* $\hat{\mathcal{P}} = \{\hat{x}\}$. The $\text{renorm}()$ function considers the re-normalization of features that is needed if points in $\mathcal{C}1$ and $\mathcal{C}2$ went through different normalization processes according to Eq.(3). In other words, $\text{renorm}()$ transforms the space defined by the centroids obtained by two different snapshots in a common hypercube space of unitary side. This normalization step is required since normalizing over all snapshots is not possible because in an online analysis system future snapshot are not known a priori. In our case, assuming $\mathcal{C}1 = \mathcal{C}^{(n)}$, $\mathcal{C}2 = \mathcal{C}^{(n+1)}$, from Eq.(3) for each $m \in \mathcal{M}$ we have:

$$\text{Min}_m = \min \left(\min_m^{(n)}, \min_m^{(n+1)} \right) \quad (7)$$

$$\text{Max}_m = \max \left(\max_m^{(n)}, \max_m^{(n+1)} \right) \quad (8)$$

$$\text{renorm}_m(a) = \frac{a - \text{Min}_m}{\text{Max}_m - \text{Min}_m} \quad (9)$$

To better explain the need of this two-step normalization process we describe a simple one-dimensional example. Consider the case in which the first snapshot has values varying in $[0, 15]$, and the second snapshot in $[2, 22]$. We first perform a per-snapshot normalization to run DBSCAN, so that we obtain $[0, 15] \rightarrow [0, 1]$ as by Eq.(3). Similarly $[2, 22] \rightarrow [0, 1]$ for the second snapshot. Next, to compare these two snapshots, the $\text{renorm}()$ function will re-normalize the space in a common space with $[0, 22] \rightarrow [0, 1]$.

2) *Centroid Distance*: Given a centroid \hat{x} and a centroid pattern $\hat{\mathcal{P}}$, we define the *Centroid Distance (CD)* as the distance between \hat{x} and its closest centroid in $\hat{\mathcal{P}}$. Specifically, we compute the closest centroid $\hat{y}^* \in \hat{\mathcal{P}}$ such that $d(\hat{x}, \hat{y}^*) \leq d(\hat{x}, \hat{y}) \forall \hat{y} \in \hat{\mathcal{P}}$. $d(x, y)$ can be any distance metric that is valid in the feature space. In this work, we use the classic Euclidean distance. Thus, the Centroid Distance CD of the centroid \hat{x} from centroids in $\hat{\mathcal{P}}$ is

$$CD(\hat{x}, \hat{\mathcal{P}}) = \min_{\hat{y} \in \hat{\mathcal{P}}} d(\hat{x}, \hat{y}) \quad (10)$$

Hence, the Centroid Distance couples centroids according to a nearest neighbor principle.

3) *Pattern Dissimilarity*: At last, we define the *Pattern Dissimilarity - PD* - as the sum of the Centroid Distance among every centroid in the clusterings. Since the number of clusters in $\hat{\mathcal{P}}1$ and $\hat{\mathcal{P}}2$ may be different, we need to symmetrize the definition:

$$PD(\hat{\mathcal{P}}1, \hat{\mathcal{P}}2) = \sum_{\hat{x} \in \hat{\mathcal{P}}1} CD(\hat{x}, \hat{\mathcal{P}}2) + \sum_{\hat{x} \in \hat{\mathcal{P}}2} CD(\hat{x}, \hat{\mathcal{P}}1) \quad (11)$$

Fig. 6 depicts the *Pattern Dissimilarity* computation considering a 2-dimensional space. From left to right, DBSCAN first clusters the points (grey dots for the first snapshot, white for

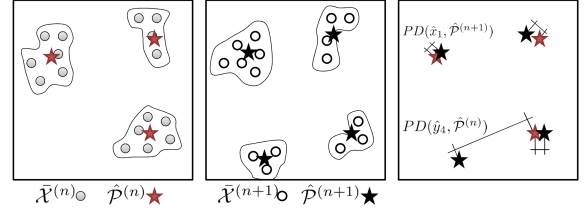


Fig. 6: Example of Clusterings, Patterns and Centroid Distance computations.

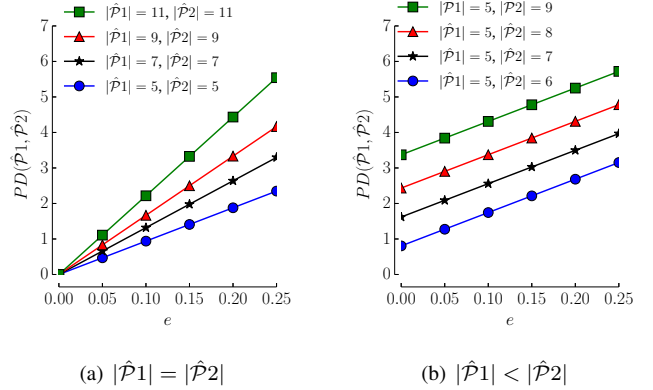


Fig. 7: *Pattern Dissimilarity* for increasing noise e , for constant and increasing number of centroids.

the second). Then, centroids emerge to form the patterns, and we compute the Centroid Distance for each centroid. Finally, the *Pattern Dissimilarity* is the sum of all Centroid Distances.

In the following, we consider two subsequent snapshots n , and $n+1$, compute the clustering $\mathcal{C}^{(n)}$ and $\mathcal{C}^{(n+1)}$, then extract the patterns $\hat{\mathcal{P}}^{(n)}$ and $\hat{\mathcal{P}}^{(n+1)}$, and finally compute their dissimilarity $PD(\hat{\mathcal{P}}^{(n)}, \hat{\mathcal{P}}^{(n+1)})$.

We note that we can base the *Pattern Dissimilarity* on other similarity metrics different from the Euclidean distance, e.g., the well known Cosine Similarity. However, as we show in Sec. IV-C using the Euclidean distance lets the *Pattern Dissimilarity* to inherit linear properties, and therefore to vary proportionally with size of the changes. Observe also that the design of the *Pattern Dissimilarity* offers a nice property that is particularly desirable for troubleshooting purposes. In particular, the *Pattern Dissimilarity*, which is a simple sum of Euclidean distances, lets us immediately pinpoint the centroids responsible for changes in the pattern. As we show in Sec. VI, this aspect is crucial, as it allows us to design an automatic procedure that i) captures changes in YouTube CDN infrastructure, and ii) highlights the edge-nodes involved in these changes.

C. Observations about the Pattern Dissimilarity

We run some numerical evaluation to gauge how the *Pattern Dissimilarity* changes with respect to changes in the input data. We consider two main sources of changes: i) centroids that simply move from their position, and ii) the birth of new

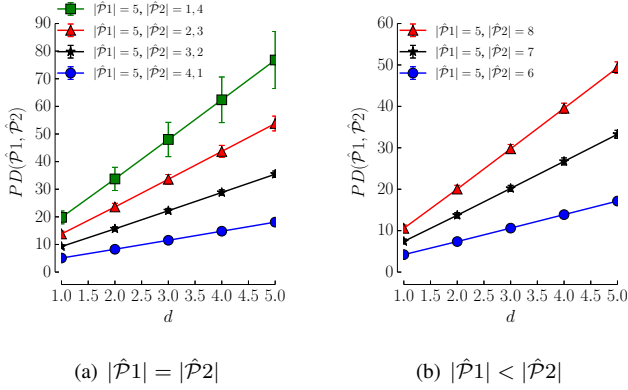


Fig. 8: *Pattern Dissimilarity* for increasing distance among clusters d , for constant and increasing number of centroids.

centroids reflecting the generation of a new cluster in the data.

1) *Changes within the same metric space:* Consider first that case where changes to samples leave samples within the same metric space, i.e., $\min_m^{(n)} = \min_m^{(n+1)}$ and $\max_m^{(n)} = \max_m^{(n+1)}$.

For the first scenario, we generate a random pattern $\hat{C}1$ of $N = |\hat{C}1|$ centroids. We randomly place centroids in the unitary hypercube of edge 1 in \mathbb{R}^N according to a uniform distribution. Then, we generate pattern $\hat{C}2$ by taking the centroids in $\hat{C}1$, and repositioning them in a random sphere of radius e centered in the centroid original position. Finally, we compute $PD(\hat{C}1, \hat{C}2)$. We repeat the experiment for 100 times, and compute the average and standard deviation of the obtained values. Fig. 7(a) reports the average *Pattern Dissimilarity* and its standard deviation for increasing values of e , and for different values of N . As expected, curves pass through the origin, and linearly grow with e . The larger is N , the higher is the average *Pattern Dissimilarity* and its standard deviation.

For the second case, we run the same experiment while also increasing the number of centroids. Thus $|\hat{C}1| < |\hat{C}2|$. Fig. 7(b) shows the results. Notice the nice property of the *Pattern Dissimilarity* for which the birth of new centroids causes the *Pattern Dissimilarity* to grow by a factor that is proportional to the number of new centroids. This is due to definition in Eq.(11) in which no normalization is present. This property is important, as it lets the *Pattern Dissimilarity* nicely highlight the sudden birth (or death) of centroids i.e., edge-nodes in our scenario.

2) *Changes to a larger metric space:* Consider now the that case where changes move part of the samples outside the metric space at time n . In particular, let samples move/appear with $\max_m^{(n+1)} = d \max_m^{(n)}$, $d > 1$.

Fig. 8 shows results. Starting with left plot, we consider the case where 5 clusters are present at both time. At time $n + 1$, points of k clusters move in a different portion of the space, being allowed to move is a space of diameter d bigger than the original one. Results show that this change has a much greater

impact, see Fig. 8(a). In the figure, $|\hat{P}2| = x, y$ states that x cluster still lie in the original space, and y lie in the upscaled space. Intuitively, since points now move to a larger space, the *Pattern Dissimilarity* of the cluster which lies outside the original space let the *Pattern Dissimilarity* grow higher.

Fig. 8(b) consider the birth of new clusters, which lie in the upscaled space of factor d . Also in this case, the *Pattern Dissimilarity* grows much higher than when considering the birth of clusters within the same space – cfr. Fig 7(b).

These simple experiment allows us also to select thresholds to highlight important changes, rather than minor changes. For instance, when samples move outside the original space, the *Pattern Dissimilarity* is typically larger than 10. Conversely, when changes move samples within the same space, *Pattern Dissimilarity* is smaller than 10. This will be useful when highlighting significant changes in real data.

D. Complexity

After evaluating different aspects of the methodology, the last important part to analyze is its complexity. This step is required to understand the feasibility of running *YouLighter* in a real environment. To evaluate *YouLighter* complexity we study the computational cost of the different steps. We assume that the network has been instrumented to extract flow level logs from passive observations of packets. In our work we rely on Tstat a tool developed at Politecnico di Torino able to perform live traffic monitoring up to few Gb/s using off-the-shelf hardware [23], [27].

Assume to have N caches and a total number of YouTube flows F . From our dataset, we always obtain N in the order of 1,000 and F amounting to half billion flows in each week of data from ISP1. Therefore, a one week long dataset can be easily stored in memory of MB magnitude. Given the flow level log, the first step consists in measurement consolidation. It consists in grouping flows by cache and filter less used ones. Using an hash-based data structure where the key is the cache IP address, counting flows per cache has a complexity of $O(F)$.

The second step consists in feature extraction and data normalization for each flow. For each cache, empirical percentiles must be computed which entails sorting of flows. Worst case complexity is $O(F \ln(F))$ when $N = 1$ and all flows belong to the same cache. Assuming instead that F flows are equally split among N caches, the complexity becomes $O(N \frac{F}{N} \ln(\frac{F}{N})) = O(F \ln(\frac{F}{N}))$.

The third step is running DBSCAN. According to authors in [6], the algorithm complexity is $O(N \ln(N))$. The output consists in M clusters. The final step consists in computing the *Pattern Dissimilarity*. Firstly, it requires to compute the boundary values for the *renorm* function. This operation is linear $O(N)$ since it requires to find the minimum and maximum values of features. Secondly, it computes the *centroid* of each pattern. For each the M patterns, each containing L caches, we have a complexity of order $O(ML)$. Assuming L to be $O(\frac{N}{M})$, the complexity reduces to $O(N)$. The next part has to deal with the centroid distance. This part has a computational complexity of $O(M^2)$. Finally the *Pattern*

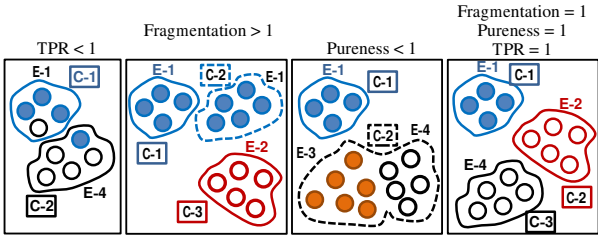


Fig. 9: Examples of patterns for which the *True Positive Rate*, the *Fragmentation Index*, and the *Pureness Index* are not equal to 1, and the optimal case in which they are all equal to 1. Color represent the GT-label.

Dissimilarity is computed with a cost of $O(M)$ since we have to sum all pattern distances. Overall, *YouLighter* complexity is thus dominated by the second step, i.e., $O(F \ln(\frac{F}{N}))$. For our *YouLighter* implementation, we used *Python* program language which took on average less than two minutes to perform all computation for one week of data.

V. DBSCAN PERFORMANCE

In this section we first assess and tune the performance of DBSCAN in order to identify edge-nodes. We next run *YouLighter* over a longitudinal dataset to show its ability to highlight sudden changes in the YouTube CDN.

A. Clustering Performance Metrics

We first evaluate the impact of the parameter settings on the DBSCAN results. In particular, we aim to understand how good is the matching between the clustering DBSCAN returns and the edge-nodes we observe in the measurements. To perform this analysis, we consider the snapshot X from November 4th to November 10th, 2013, in trace *ISP1-A*. We manually inspect the dataset, and, guided by the IATA codes, we assign each cache a label corresponding to the edge-node in the YouTube CDN. We manually cross-check labels by inspecting server IP addresses and subnets, RTT and TTL distributions to verify the accuracy of the labels. The result is a ground truth label, GT-label, that we assign to each cache. In total we find $|X| = 620$ caches serving more than $MinFlow = 50$ flows, and belonging to 6 edge-nodes, each identified by a different GT-label. Hence, the number of GT-labels is $N_{GT} = 6$.

We then run DBSCAN as described in Sec. IV-A, obtaining the clustering \mathcal{C} . Let $N_C = |\mathcal{C}|$ be the number of clusters. We next use the GT-labels to assign a label to caches by using a majority-voting scheme: For each cluster $C_j \in \mathcal{C}$, we assign all caches $x \in C_j$ the most frequent GT-label observed in C_j . Caches whose assigned label matches the GT-label are the so called True Positives (TP), whose number is N_{TP} . Conversely, caches whose assigned label is different from their GT-label are False Positives (FP), whose number is N_{FP} . $|X| = N_{TP} + N_{FP}$. We compute the set of distinct labels assigned to clusters in \mathcal{C} , whose number is $N_L \leq N_{GT}$. We do not assign any label to the caches which DBSCAN classifies as noise points.

To validate the clustering we obtain with DBSCAN we consider three different indices, as follows:

$$TPR = \frac{N_{TP}}{|X|}, \mu = \frac{N_C}{N_L}, \phi = \frac{N_L}{N_{GT}} \quad (12)$$

- 1) The True Positive Rate ($TPR \leq 1$), also known in the literature as “Purity” [26] measures the ratio between TP and the number of samples in the experiment. $TPR = 1$ means that all labels are identical to the GT-label. $TPR < 1$ indicates the presence of i) mislabeled caches (or FP), or ii) noise points (unlabeled points). Leftmost sub-figure in Fig. 9 reports a simple example where the clustering algorithm mislabels a cache for both the GT-labels E-1 and E-4, thus leading to $TPR < 1$. Colors represent the GT-label.
- 2) The *Fragmentation Index* ($\mu \geq 1$) is a custom metric that captures the case when more clusters share the same GT-label. When $\mu = 1$, the number of clusters is identical to the number of GT-labels and DBSCAN assigns each cluster a different GT-label. When $\mu > 1$ instead, we have more clusters which share the same GT-label, i.e., DBSCAN splits an edge-node into two or more clusters. Second sub-figure in Fig. 9 reports an example where the clustering algorithm splits edge-node E-1 in two different clusters, C-1 and C-2, thus leading to $\mu > 1$.
- 3) *Pureness Index* ($\phi \leq 1$) is also a custom metric that measures the ability to identify all edge-nodes. When $\phi = 1$, DBSCAN assigns each GT-label to at least one cluster, i.e., it correctly identifies all edge-nodes. $\phi < 1$ indicates that some edge-nodes disappear into other clusters (i.e., their GT-label is not the majority label for any cluster). Third sub-figure of Fig. 9 reports an example where the clustering algorithm groups together edge-nodes with GT-labels E-3 and E-4 in cluster C-2, thus leading to $\phi < 1$.

Rightmost sub-figure in Fig. 9 also depicts the ideal clustering result in which DBSCAN groups correctly the caches for all the edge-nodes, i.e., one cluster for each GT-label (edge-node), leading to the case in which all the clustering performance indices, TPR , μ and ϕ , are equal to 1.

Finally, we use also the number of noise points as an index of bad clustering results, i.e., the inability of DBSCAN to group caches into edge-nodes.

B. DBSCAN Performance and Parameter Sensitivity

We run experiments to evaluate the impact of DBSCAN parameters, i.e., the choice of the features, $MinPts$ and ϵ . For now, we set features as the 20th, 35th, 50th, 65th, 80th percentiles for both the RTT and TTL distributions. $MinPts$ is typically not critical since it defines the minimum number of caches in an edge-node DBSCAN needs to form a cluster. We set it to 5. Instead, we must choose ϵ carefully: If too small, a lot of fragmented clusters will emerge, or a large number of points will not be able to form dense areas, increasing the number of noise points; conversely, large values tend to create

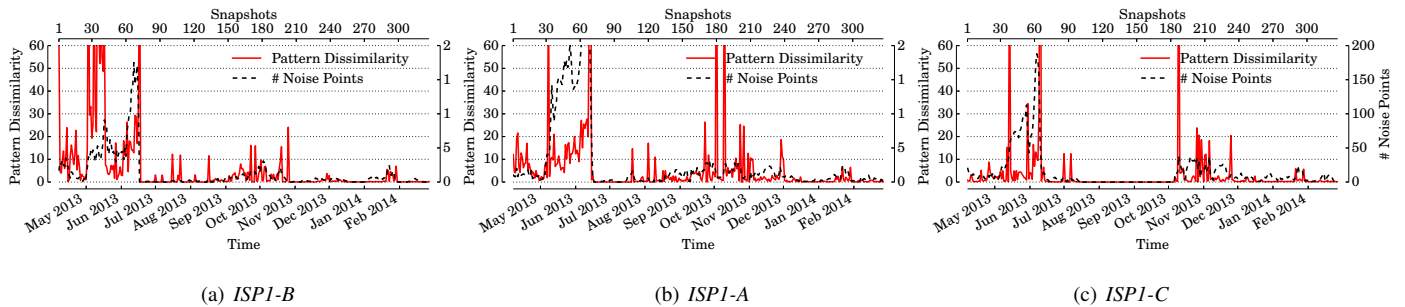
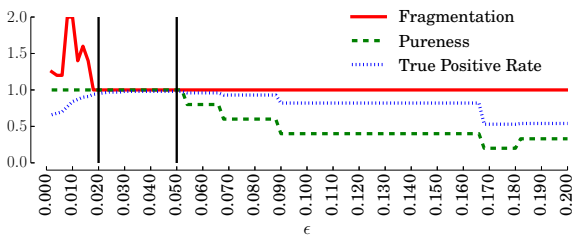
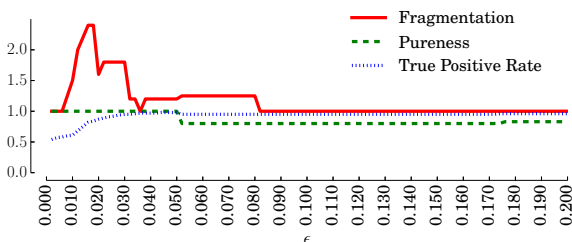


Fig. 10: *Pattern Dissimilarity* values and number of noise points for different traces from ISPI.



(a) DBSCAN with percentiles as features.



(b) DBSCAN with mean and standard deviation as features.

Fig. 11: DBSCAN with different feature settings. Performance versus ϵ . 1st week of November, *ISPI-A*.

few, very large clusters, that aggregates caches from different edge-nodes.

Fig. 11(a) reports the clustering indices when varying $\epsilon \in [0.0 : 0.2]$. As shown, we achieve the best performance with values between 0.018 and 0.052 (in between the vertical solid lines). For such values, all the three indices are equal or very close to 1. Smaller values of ϵ increase the number of noise points and artificially fragment edge-nodes into multiple clusters. TPR decreases, while μ first increases, then decreases due to caches DBSCAN labels as noise (more than 300 caches fall in the noise for $\epsilon < 0.005$). For ϵ larger than 0.052 DBSCAN merges edge-nodes into too few clusters, and both ϕ and the *TPR* considerably decrease.

We repeat this analysis for other traces and for different snapshots. We find $\epsilon \in [0.02 : 0.045]$ to give consistent results. In the following we choose $\epsilon = 0.04$.

We also run a set of experiments to choose which features to use to capture the RTT and TTL distributions. We replace the

vector of percentiles $P_m(x)$ in Eq.(3) with simple statistics, e.g., the mean and the standard deviation. The goal of this experiment is to verify whether we can replace the percentiles with some measure which does not require us to build an empirical distribution, a task which requires to collect a fairly large number of flows per cache.

Fig. 11(b) depicts results for varying ϵ . Unfortunately, DBSCAN shows a good clustering for a tiny interval of values of ϵ , e.g., $\epsilon = 0.035$. For $\epsilon > 0.035$, DBSCAN merges edge-nodes together, so that $\mu > 1$ and $\phi < 1$. By investigating further, we observe that the mean and standard deviation vary widely among caches in the same edge-node. This variability is due to the tails of the distributions which include outliers, e.g., very large RTT samples which bias the mean and standard deviation, but have little or no impact on the percentiles. Indeed, the percentiles of caches in the same edge-node are very similar, except those that gauge the tail (see the 95th percentiles in Fig.5). This suggests that the choice of the percentiles to populate the vector $P_m(x)$ is more robust with respect to other simpler statistics. We run other experiments with different percentile choices that we do not report for the sake of brevity. We observe no significant differences if we avoid considering percentiles in the tail. Similarly, we observe that using both RTT and TTL gives better results than considering RTT or TTL alone.

VI. YOULIGHTER'S HIGHLIGHTING CAPABILITY

In this section we run *YouLighter* over the four traces in Tab. I to validate its capability of highlighting changes in the YouTube CDN. The rationale is to let the ISP observe macroscopic changes that may affect a large number of users, and which may last for moderate time periods. We consider $\Delta T = 7$ days, and we start a new snapshot at midnight of every day. The choice of the time granularity is driven by the nature of the anomalies that the ISP would like to highlight. Indeed, with too small time scales, e.g., order of hours, more alarms would be possibly raised due to the natural control system of CDNs. At the same time, an anomaly that lasts order of hours would possibly be not relevant for end-users, since the system would return to normality in short time. Snapshots form a sliding window that moves forward every day, and aggregates statistics for the past seven days. $\Delta T = 7$ days guarantees us to obtain a statistically significant

amount of feature measurements for each of the caches in the set responsible of carrying the 90% of traffic.

Fig. 10 shows the evolution of the *Pattern Dissimilarity* (red solid curve, left y-axes) over time. It also depicts the evolution over time of the number of caches that remain in the noise after clustering (black dashed curve, right y-axes). From left to right, plots refer to *ISPI-B*, *ISPI-A* and *ISPI-C*. X-axes reports daily snapshots, starting from April 1st, 2013.⁷

As shown, the *Pattern Dissimilarity* is very good at highlighting events. Indeed, according to Sec. IV-C, a $PD > 10$ suggests that the clustering at time (n) is very different to the one at time ($n + 1$). Thanks to the data aggregation we obtain with the clustering, we can easily analyze the highlighted events, and quickly identify the edge-nodes involved in the changes. We investigate these events, and verify that they all correspond to sudden changes in the edge-nodes used by YouTube in serving ISP customers. In the following, we illustrate the most relevant ones, i.e., those with a $PD > 50$.

A. Large event, involving all ISP customers

We first investigate an event *YouLighter* highlights in three different datasets. It starts on May 2nd (snapshot 27), May 7th (snapshot 32), and May 13th (snapshot 38) for *ISPI-B*, *ISPI-A* and *ISPI-C*, respectively. *Pattern Dissimilarity* peaks above 60. Starting from then, both PD and the number of noise points are very large. This indicates an unstable behavior, with many caches that DBSCAN cannot successfully group together, and the clustering pattern that keeps changing day by day, for more than 40 days.

To give the intuition of what happened, top plot of Fig. 12 shows the per-cache percentiles of the RTT that we measure in *ISPI-A* before, during, and after the anomalous event. First, we notice that most of the edge-nodes suddenly change: E-1, E-4, E-5 and E-6 actually “disappear” from the clustering pattern, and during the event, many previously unseen caches in edge-node E-2 start serving lots of customers (observe the center plot). Second, and more surprisingly, the path properties to these new caches is by far different from paths to other caches in E-2: the RTT percentiles are much larger (95ms versus 15ms for the 50th percentile) and much more variable. Despite these caches share the same IATA code (E-2), *YouLighter* identifies two clusters since the path to reach caches differs. This is clearly shown by the RTT percentiles, which makes them like to be in two different locations, with the former possibly being severely congested. We call these new cluster Bad-E-2, in opposition to caches showing small RTT, i.e., Good-E-2. While RTT distribution clearly allows us to identify a sudden CDN change, the TTL measurements in the bottom plot of Fig. 12 does not reveal any additional information with respect to what RTT already does.

We now analyze the impact of such change on the Quality of Experience the ISP customers perceive. We report in Fig. 13 the distributions of the download throughput obtained by video retrieved by caches in E-3, the best edge-node to ISP customers, Good-E-2 and Bad-E-2. The difference is striking:

⁷PoP referring to *ISPI-C* suffered an outage from mid July 2013 to the end of September.

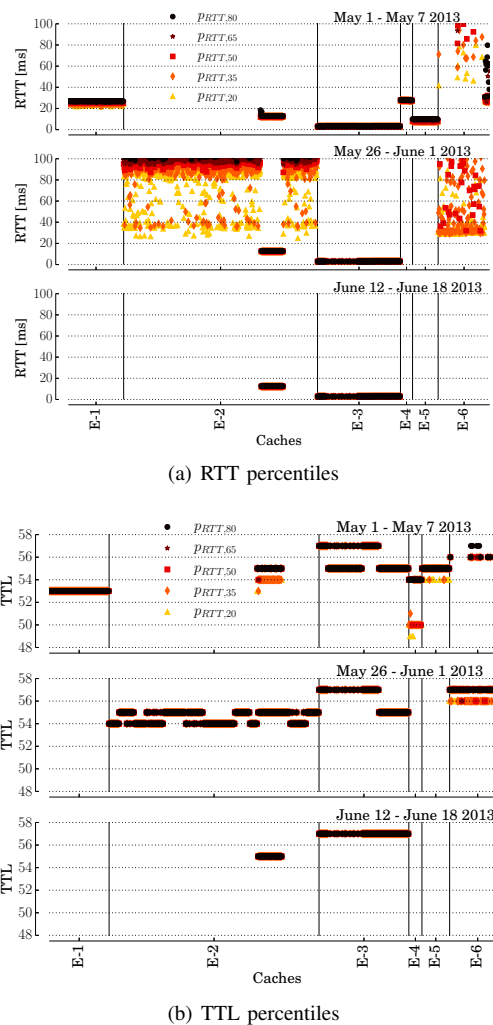


Fig. 12: Per-cache RTT and TTL percentiles during the ISP-wide anomaly in May 2013. Dataset *ISPI-A*.

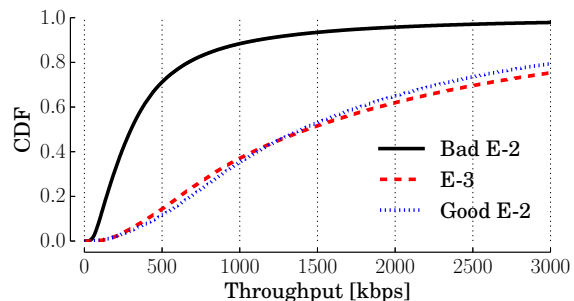


Fig. 13: Throughput distribution for flows served by E-3, Good-E-2 and Bad-E-2 during the large anomaly we observe in May 2013. Dataset *ISPI-B*.

while videos served by E-3 and Good-E-2 have throughput that allows to enjoy YouTube with no major impact on the QoE ($>1,000$ kb/s in 63% of the cases), the throughput for Bad-E-2 caches is below 500 kb/s (250 kb/s) in 75% (40%) of the cases, clearly not enough to enjoy a video with a satisfiable

Format	Good-E2	Bad-E2
144p	17.4%	31.7%
240p	18.3%	26.1%
360p	45.4%	35.7%
480p	14.5%	5.3%
720p	3.8%	1.0%
1080p	0.6%	0.2%
AAC128	80.3%	92.0%
AAC256	19.7%	8.0%

TABLE II: Fractions of video and audio DASH formats served by Good-E-2 and Bad-E-2. Dataset *ISP1-B*.

QoE [28]. Tab. II corroborates above observation reporting the fractions of video (and audio) formats seen in flows handled by both Good-E-2 and Bad-E-2.⁸ For this analysis we consider only DASH formats, as for these formats the cache delivering the video automatically adapts the quality of the video stream depending on the congestion it measures on the path to the client. As shown, Good-E-2 serves larger fractions of high-definition videos. Conversely, the share of videos encoded with low-definition (144p and 240p) increases for Bad-E-2. This confirms that Bad-E-2 experienced possible congestion during the monitored period, severely impairing the QoE of the users.

By double checking this event with the ISP network support team, we confirm the incident involved most of their customers, increasing dramatically the complaining at their customer support. This confirms the pervasiveness of this event upon ISP customers.

The accident reported above is an example which testifies that changes in the CDN may raise issues in the video delivery, finally harming users’ experience. This highlights how important for the ISP is to monitor and pinpoint changes in the YouTube CDN. The task of measuring how the variability of the CDN structure may impact on the QoE perceived by the users is beyond the focus of this paper.

B. Other events for ISP1

We manually cross check other events, and find that some of those affected only part of the ISP customers. This shows that YouTube CDN allocates customers to edge-nodes using a fine grained granularity, i.e., the load-balancing allows to identify small groups of clients by using the client IP address (or network). For instance, on October 2nd (snapshot 180) and October 9th (snapshot 187) *YouLighter* highlights two sudden changes in the *ISP1-A* and *ISP1-C*, as the *Pattern Dissimilarity* peaks over 60. Inspecting the astral distances one by one, we observe that the changes are due to 3 edge-nodes (E-4, E-5 and E-6) out of 7 that suddenly “appear” in snapshot 180 and “disappear” in snapshot 187. The remaining four edge-nodes then serve the videos for customers in *ISP1-A* and *ISP1-C*. We analyze the impact of the presence of such caches on the QoE by measuring the aggregate download throughput before,

⁸Observe that in our dataset only a tiny portion ($\sim 1\%$) of requests are HTTPS, and, thus, encrypted. For the wide majority of the cases, the information about video and audio formats are exposed in plain text in HTTP requests.

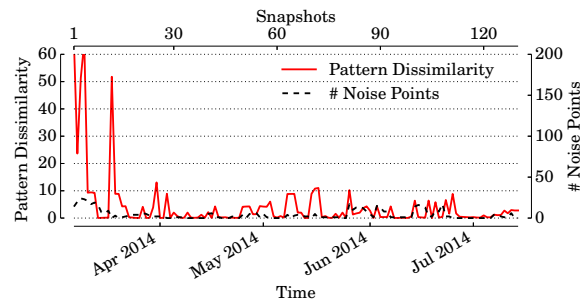


Fig. 14: *Pattern Dissimilarity* values and number of noise points for dataset *ISP2*.

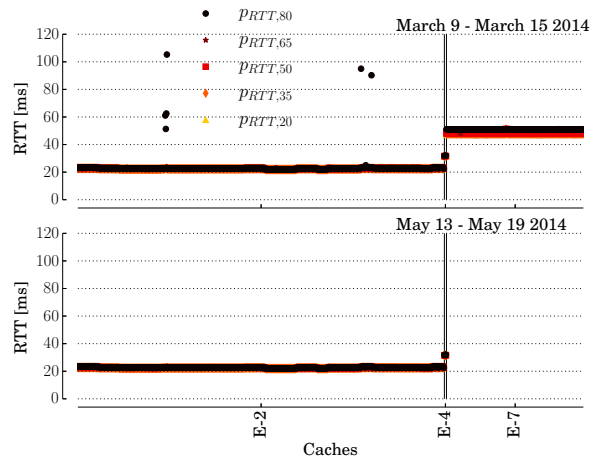


Fig. 15: Per-cache RTT percentiles during the second ISP-wide anomaly in March 2014. Dataset *ISP2*.

during and after their permanence, but we do not appreciate any significant change. Also in this case we double check the event with the ISP support team and we confirm that the change had no influence on the QoE as the customer support did not receive any meaningful complaining in the considered period.

C. Events in ISP2

As a last set of experiments, we run *YouLighter* on the *ISP2* dataset, which we recall we collect in *ISP2*, a different ISP in a different country. We run *YouLighter* with the same parameters we tune for *ISP1*, i.e., without going through ϵ optimization. Indeed we aim to check whether if the edge-node model that DBSCAN creates is general and robust enough to work in a completely different scenario.

We repeat the experiment of Fig. 10 for *ISP2* dataset, and we analyze the evolution of the *Pattern Dissimilarity* and number of noise points. We report the results in Fig. 14. To check if the clustering correctly identifies the edge-nodes, we select five different snapshots at random among the ones where *YouLighter* highlights no events. Again, we use the IATA codes as ground truth, and we manually check IP address subnets, RTTs and TTLs to see if some suspicious cache is present in a cluster. The clustering results in perfect match with the

(possible) edge-nodes in the ground truth. This despite edge-nodes, path, and ISP in this dataset are completely different.

We then check two suspicious events. The first one occurs from March 7th to March 10th, 2014 (snapshots 1-4, $PD > 60$), and the second one happens on March 18th, 2014 (snapshot 12, $PD > 50$). We observe that the first anomaly is due to a change in the network path to reach a small group of caches in E-2. We observe that this deviation does not influence the QoE perceived by the users. For the second event, by comparing the clustering at snapshot 12 with the following snapshot, i.e., snapshot 13 (March 19th), we observe a notable change in the infrastructure of the YouTube CDN: as depicted in Fig. 15 which compares the per-cache RTT percentiles, all caches belonging to edge-node E-7 disappear. Also in this case, the change has no evident impact on users' QoE, as the average download throughput does not vary. However, we notice that the edge-node E-7 represents a much more expensive route for the ISP2, since it is located in an remote ISP for which no peering agreements are in place.

VII. COUNTERMEASURES

In this section, we present some possible techniques that ISPs may consider to this end, leaving a thorough design and analysis for future work.

Firstly, ISPs position allows them to partially control the network routing of traffic. Thus, ISPs may employ traffic engineering techniques to control YouTube traffic using both intra- and inter-routing algorithm. By using BGP, ISPs may reduce congestion by redistributing traffic among different peering links [29]. By announcing via BGP reachability of their network through other Autonomous System (AS) the ISP can influence YouTube cache allocation policy as well. For instance, ISP1 used this technique to mitigate problems highlighted in Fig. 13. In that specific case, ISP1 forced its AS number to be seen as reachable through another ISP (ISP2), located in a different country. This caused YouTube CDN to change the cache allocation policy so that customers from the ISP1 were directed to a edge-node located in the ISP2 country. YouTube traffic was then coming from ISP2 to ISP1, through a high-capacity and uncongested peering link, de facto solving the congestion problem.

A second and more controversial solution would be using DNS directly. By enforcing policies on its DNS servers, the ISP may force a video request to be served by a specific edge-node or even by a specific cache, overruling the decision of the YouTube CDN. As explained in Sec. III-B, as soon as a client requests a video, YouTube selects a cache and returns the cache hostname to the client e.g. `r7---fra07t16.c.youtube.com`. After receiving this hostname the client sends a DNS query to the DNS server (typically managed by the ISP) to retrieve the IP address of the hostname. As a consequence, in case the ISP knows that `r7---fra07t16.c.youtube.com` performance are poor, the ISP DNS can return the IP address of a different cache. This is possible since according to [3], [4], any cache can serve any video. This solution, allows the ISP to select which cache has to manage each request. Therefore the ISP

may potentially override YouTube load balancing policies. Some drawbacks have to be faced. First, even if previous studies discovered that any cache can serve any video, the ISP can not be sure that its choice will not introduce a bigger latency due to cache miss, that can cause a further redirection to other caches. Second, the ISP can not control whether a cache will be switched off for maintenance. Observe that an ISP attempt to react to changes in the CDN infrastructure could cause further reactions on YouTube's side too. As such, careful investigations must be done to design and study this kind of policies.

VIII. CONCLUSIONS

In this paper we proposed a novel system, named *YouLighter*, that leverages passive observation of network traffic and unsupervised machine learning techniques to automatically monitor and identify changes in the YouTube CDN. Based on the well known DBSCAN clustering algorithm, *YouLighter* is able to automatically group thousands of caches into few edge-nodes. To then compare the results of clustering obtained considering different snapshots collected in consecutive time intervals, we propose the *Pattern Dissimilarity* which allows to easily pinpoint changes in clusters.

YouLighter is validated using a large dataset of traces reporting the activity of users regularly accessing YouTube. Our results are excellent: we show that after a short and simple tuning procedure to find the best setup for DBSCAN, *YouLighter* can detect anomalous events that happened in YouTube CDN. For instance, we could notice a large transformation in a crucial edge-node of YouTube CDN which notably impaired the QoE perceived by the monitored ISP customers for more than 40 days.

We believe that *YouLighter* may represent a promising opportunity for ISPs, network administrators, developers and researchers to monitor the traffic generated by YouTube CDN. ISPs, for instance, may employ *YouLighter* to design automatic traffic engineering policies or to promptly react when changes in YouTube CDN impair the QoE of their customers.

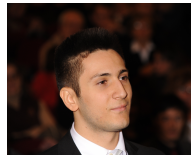
Our ongoing efforts are focused on three directions: First, we are working to automate the tuning of *YouLighter*'s parameters, and, thus, its whole operation process. Second, we are developing an online deployment of *YouLighter*, capable of detecting changes in YouTube CDN in real time. Third, we are adapting it to consider other use cases.

REFERENCES

- [1] M. Calder, X. Fan, Z. Hu, E. Katz-Bassett, J. Heidemann, and R. Govindan. Mapping the expansion of google's serving infrastructure. In *ACM IMC*, 2013.
- [2] V. Adhikari, S. Jain, Y. Chen, and Z.-L. Zhang. Vivisecting youtube: An active measurement study. In *IEEE INFOCOM*, 2012.
- [3] R. Torres, A. Finamore, J. R. Kim, M. Mellia, M. Munafo, and S. Rao. Dissecting video server selection strategies in the youtube cdn. In *IEEE ICDCS*, 2011.
- [4] P. Casas, P. Fiadino, and A. Bär. Understanding http traffic and cdn behavior from the eyes of a mobile isp. In *PAM*, 2014.
- [5] P. Casas, A. D'Alconzo, P. Fiadino, A. Bar, A. Finamore, and T. Zseby. When youtube does not work: Analysis of qoe-relevant degradation in google cdn traffic. *Network and Service Management, IEEE Transactions on*, 11(4):441–457, Dec 2014.

- [6] M. Ester, H.-P. Kriegel, J. Sander, and X. Xu. A density-based algorithm for discovering clusters in large spatial databases with noise. In *ACM KDD*, 1996.
- [7] T. Hossfeld, R. Schatz, E. Biersack, and L. Plissonneau. Internet video delivery in youtube: From traffic measurements to quality of experience. In *Data Traffic Monitoring and Analysis*, volume 7754, pages 264–301. Springer, 2013.
- [8] A. Patcha and J.-M. Park. An overview of anomaly detection techniques: Existing solutions and latest technological trends. *Comput. Netw.*, 51(12):3448–3470, Aug. 2007.
- [9] V. Chandola, A. Banerjee, and V. Kumar. Anomaly detection: A survey. In *Computing Surveys*, volume 41, pages 1 – 58. ACM, 2009.
- [10] H. Yan, A. Flavel, Z. Ge, A. Gerber, D. Massey, C. Papadopoulos, H. Shah, and J. Yates. Argus: End-to-end service anomaly detection and localization from an isp’s point of view. In *IEEE INFOCOM*, 2012.
- [11] A. Lakhina, M. Crovella, and C. Diot. Mining anomalies using traffic feature distributions. *SIGCOMM Comput. Commun. Rev.*, 35(4):217–228, Aug. 2005.
- [12] J. Jiang, V. Sekar, I. Stoica, and H. Zhang. Shedding light on the structure of internet video quality problems in the wild. In *Proceedings of the Ninth ACM Conference on Emerging Networking Experiments and Technologies*, CoNEXT ’13, pages 357–368, New York, NY, USA, 2013. ACM.
- [13] P. Fiadino, A. D’Alconzo, A. Bar, A. Finamore, and P. Casas. On the detection of network traffic anomalies in content delivery network services. In *Teletraffic Congress (ITC), 2014 26th International*, pages 1–9. IEEE, 2014.
- [14] G. Münz, S. Li, and G. Carle. Traffic anomaly detection using k-means clustering. In *GI/ITG Workshop MMBnet*, 2007.
- [15] R. D. Torres, M. Y. Hajjat, S. G. Rao, M. Mellia, and M. M. Munafò. Inferring undesirable behavior from p2p traffic analysis. In *SIGMETRICS Performance Evaluation Review*, volume 37, pages 25 – 36. ACM, 2009.
- [16] D. Chakrabarti, R. Kumar, and A. Tomkins. Evolutionary clustering. In *Proceedings of the 12th ACM SIGKDD International Conference on Knowledge Discovery and Data Mining*, KDD ’06, pages 554–560, New York, NY, USA, 2006. ACM.
- [17] C. C. Aggarwal, J. Han, J. Wang, and P. S. Yu. A framework for clustering evolving data streams. In *Proceedings of the 29th International Conference on Very Large Data Bases - Volume 29*, VLDB ’03, pages 81–92. VLDB Endowment, 2003.
- [18] M. K. Goldberg, M. Hayvanovych, and M. Magdon-Ismail. Measuring similarity between sets of overlapping clusters. In *IEEE SocialCom*, 2010.
- [19] P. Kalnis, N. Mamoulis, and S. Bakiras. On discovering moving clusters in spatio-temporal data. In *Advances in spatial and temporal databases*, volume 37, pages 364 – 381. Springer, 2005.
- [20] Z. Li, B. Ding, J. Han, and R. Kays. Swarm: Mining relaxed temporal moving object clusters. In *Proceedings of the VLDB Endowment*, volume 3, pages 723–734. VLDB Endowment, 2010.
- [21] D. Kifer, S. Ben-David, and J. Gehrke. Detecting change in data streams. In *ACM VLDB*, 2004.
- [22] D. Giordano, S. Traverso, L. Grimaudo, M. Mellia, E. Baralis, A. Tongaonkar, and S. Saha. Youlighter: An unsupervised methodology to unveil youtube cdn changes. In *27th International Teletraffic Congress*, 2015.
- [23] A. Finamore, M. Mellia, M. Meo, M. M. Munafò, and D. Rossi. Experiences of internet traffic monitoring with tstat. *Network, IEEE*, 25(3):8–14, 2011.
- [24] D. Naylor, A. Finamore, I. Leontiadis, Y. Grunenberger, M. Mellia, M. Munafò, K. Papagiannaki, and P. Steenkiste. The cost of the s in https. In *Proceedings of the 10th ACM International on Conference on emerging Networking Experiments and Technologies*, pages 133–140. ACM, 2014.
- [25] I. N. Bermudez, M. Mellia, M. M. Munafò, R. Keralapura, and A. Nucci. Dns to the rescue: Discerning content and services in a tangled web. In ACM, editor, *IMC*, 2012.
- [26] P.-N. Tan, M. Steinbach, V. Kumar, et al. *Introduction to data mining*, volume 1. Pearson Addison Wesley Boston, 2006.
- [27] D. Rossi and M. Mellia. Real-time tcp/ip analysis with common hardware. In *Communications, 2006. ICC’06. IEEE International Conference on*, volume 2, pages 729–735. IEEE, 2006.
- [28] P. Casas, A. Sackl, S. Egger, and R. Schatz. Youtube amp; facebook quality of experience in mobile broadband networks. In *Globecom Workshops (GC Wkshps), 2012 IEEE*, pages 1269–1274, Dec 2012.
- [29] B. Quoitin, C. Pelsser, L. Swinnen, O. Bonaventure, and S. Uhlig. Interdomain traffic engineering with bgp. *Communications Magazine, IEEE*, 41(5):122–128, 2003.

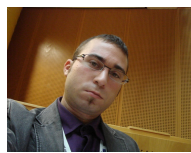
AUTHORS



Danilo Giordano received his M.Sc. Degree in Computer Engineering from Politecnico di Torino, Italy, in 2013. In 2014, he joined the Telecommunication Networks Group of Politecnico di Torino as Ph.D. Candidate. During Summer 2014, he was a research intern at Narus Inc, now part of Symantec, working on anomaly detection techniques. His research interests cover several aspects of network traffic characterization, monitoring, anomaly detection, and security on the Internet.



Stefano Traverso (M’12) Ph.D. His research interests include privacy-preserving systems, network measurements and content delivery networks. During his Ph.D. and Post-doc he has been visiting Telefonica I+D research center (Barcelona, Spain), NEC Laboratories (Heidelberg, Germany) and Alcatel-lucent Bell Labs (Paris, France). He is currently a Post-doc Fellow of the Telecommunication Networks Group of Politecnico di Torino.



Luigi Grimaudo received both his M.Sc. and Ph.D. Degree in Information and System Engineering from the Computer Engineering Department of Politecnico di Torino, Italy, in 2010 and 2013, respectively. From 2011 to 2014 he collaborated with Narus Inc working on traffic classification problems and on-line social networks analysis. His research interests cover the areas of Internet traffic classification, recommendation system, social network analysis and big data.



Marco Mellia graduated from the Politecnico di Torino with Ph.D. in Electronic and Telecommunication Engineering in 2001, where he held a position as Associate Professor. In 2002 he visited the Sprint Advanced Technology Laboratories working at the IP Monitoring Project (IPMON). In 2011, 2012, 2013 he collaborated with Narus Inc, CA, working on traffic monitoring and cyber-security system design.

He has co-authored over 250 papers published in international journals and presented in leading international conferences, all of them in the area of telecommunication networks. He participated in the program committees of several conferences including ACM SIGCOMM, ACM CoNEXT, ACM IMC, IEEE Infocom, IEEE Globecom and IEEE ICC. He is Area Editor of ACM CCR, ACM/IEEE Transactions on Networking, and IEEE Transactions on Network and Service Management.

His research interest are in area of traffic monitoring, and big data analysis. He is currently the coordinator of the mPlane Integrated Project that focuses on building an Intelligent Measurement Plane for Future Network and Application Management.



Elena Baralis received her M.Sc. in Electrical Engineering and her Ph.D. in Computer and Systems Engineering from Politecnico di Torino, where she holds a position as full professor in the Control and Computer Engineering Department since 2005. Her current research interests are in the field of database systems and data mining. More specifically, her activity focuses

on algorithms for diverse data mining tasks in a Big Data environment, and on different domains where data mining techniques find their application. She has published over 100 papers in international peer-reviewed journals and conference proceedings.



Alok Tongaonkar is a Data Scientist Director leading the Center for Advanced Data Analytics (CADA) team at Symantec Corporation. His research focuses on network security and management.

Prior to joining Symantec, Alok was a Principal Member of Technical Staff in the CTO's Office at Narus, Inc. where he led the research and development of many novel technologies in the area of network protocol reverse-engineering and pioneered automated mobile app identification techniques. He has served as a reviewer for many peer-reviewed publications such as the IEEE Transactions on Information Forensics Journal and the IEEE Internet Computing Magazine. He is a Senior Member of IEEE.



Sabyasachi Saha received his PhD in Computer Science from University of Tulsa, Oklahoma. He is Principal Data Scientist at Cyphort Inc, Santa Clara, CA. Previously, he was at Symantec, Narus

Inc. and Toyota ITC. His research interests include machine learning, data mining, artificial intelligence and network security.